HHS Public Access

Author manuscript

Exp Eye Res. Author manuscript; available in PMC 2022 January 01.

Published in final edited form as:

Exp Eye Res. 2021 January ; 202: 108397. doi:10.1016/j.exer.2020.108397.

Optimal timing for activation of Sigma 1 Receptor in the *Pde6b*^{rd10}*/J* (rd10) mouse model of retinitis pigmentosa.

Jing Wang[1,2], **Haiyan Xiao**[1,2], **Barwick Shannon**[1,2], **Yutao Liu**[1,2], **S.B. Smith**[1,2,3]

[1]Department of Cellular Biology and Anatomy, Medical College of Georgia at Augusta University, Augusta, GA.

[2]James and Jean Culver Vision Discovery Institute, Augusta University, Augusta, GA.

[3]Department of Ophthalmology, Medical College of Georgia at Augusta University, Augusta, GA

Abstract

Sigma1 Receptor (Sig1R), a pluripotent modulator of cell survival, is a promising target for treatment of retinal degenerative diseases. Previously, we reported that administration of the high-affinity, high-specificity Sig1R ligand (+)-pentazocine, ((+)-PTZ) beginning at post-natal day 14 (P14) and continuing every other day improves visual acuity and delays loss of photoreceptor cells (PRCs) in the *Pde6βrd10/J (rd10)* mouse model of retinitis pigmentosa. Whether administration of (+)-PTZ, at time points concomitant with (P18) or following (P21, P24) onset of PRC death, would prove neuroprotective was investigated in this study. *Rd10* mice were administered (+)-PTZ intraperitoneally [0.5mg/kg], starting at either P14, P18, P21 or P24. Injections continued every other day through P42. Visual acuity was assessed using the optokinetic tracking response (OKR). *Rd10* mice treated with (+)-PTZ beginning at P14 retained visual acuity for the duration of the study (~0.33 c/d at P21, ~0.38 c/d at P28, ~0.32 c/d at P35, ~0.32 c/d at P42), whereas mice injected beginning at P18, P21, P24 showed a decline in acuity when tested at P35 and P42. Their acuity was only slightly better than *rd10*-non-treated mice. Electrophysiologic function was assessed using scotopic and photopic electroretinography (ERG) to assess rod and cone function, respectively. Photopic a- and b-wave amplitudes were significantly greater in *rd10* mice treated with (+)-PTZ beginning at P14 compared with non-treated mice and those in the later-onset (+)-PTZ injection groups. Retinal architecture was visualized in living mice using spectral domain-optical coherence tomography (SD-OCT) allowing measurement of the total retinal thickness, the inner retina and the outer retina (the area most affected in *rd10* mice). The outer retina measured ~35μm in *rd10* mice treated with (+)-PTZ beginning at P14, which was significantly greater than mice in the later-onset (+)-PTZ injection groups (~25μm) and non-treated *rd10* mice (~25μm). Following the visual function studies performed in the living mice, eyes were harvested at P42 for histologic analysis. While the inner retina was largely intact in all (+)-PTZ-injection groups, there was a marked reduction in the outer retina of non-treated *rd10* mice (e.g. in the outer nuclear layer

*Please send correspondence to: Sylvia B. Smith, Ph.D. Department of Cellular Biology and Anatomy, Medical College of Georgia at Augusta University, 1120 15th Street, CB 1114, Augusta, GA 30912-2000, 706-721-7392 (phone), 706-721-6120 (fax), sbsmith@augusta.edu.

there were ~10 PRCs/100μm retinal length). The *rd10* mice treated with (+)-PTZ beginning at P14 had ~20 PRCs/100μm retinal length, whereas the mice in groups beginning P18, P21 and P24 had ~16 PRCs/100μm retinal length. In conclusion, the data indicate that delaying (+)-PTZ injection past the onset of PRC death in *rd10* mice – even by a few days – can negatively impact the long-term preservation of retinal function. Our findings suggest that optimizing the administration of Sig1R ligands is critical for retinal neuroprotection.

Keywords

retinal degeneration; rd10 mouse; Sigma 1 Receptor; pentazocine; retinitis pigmentosa; optomotry; OCT; ERG

1. Introduction

Retinal degenerations such as retinitis pigmentosa (RP) constitute a group of inherited blinding conditions that are due to loss of photoreceptor cells (PRCs). Frequently rod PRCs are lost first, followed by death of cone PRCs (Guadagni et al, 2015). Efforts to either delay rod loss or extend cone function are areas of intense investigation. Current therapies for RP are limited to palliative nutritional supplementation with retinoids, especially vitamin A. While targeted gene therapy and retinal transplantation are under intense investigation, there is an urgent need also for pharmacologically-based treatment strategies especially validation of promising molecular targets (Carullo et al, 2020).

A potential therapeutic target that has gained interest owing to its robust neuroprotective properties is sigma 1 receptor (Sig1R) (Smith et al, 2018). Sig1R is a single-pass transmembrane protein with a molecular weight of ~27kD. It is an enigmatic protein and an evolutionary isolate with no known mammalian homologs. Sig1R is a pluripotent modulator of cell survival (Su et al, 2016) and as such has been recognized as a novel target for treatment of neurodegenerative diseases (Nguyen et al, 2015). It is not surprising that this protein would be of interest as a therapeutic target in retina as well. Sig1R is abundantly expressed in retina including in cells of the ganglion cell layer, the inner nuclear layer, the inner segments of PRCs and the RPE (Ola et al, 2001). It has been localized within retinal neurons and Müller glial cells to the ER, the mitochondrial associated membrane and the nuclear membrane (Jiang et al, 2006, Mavlyutov et al, 2015). There has been a host of *in vitro* studies examining the consequences on retinal cellular stress of activating Sig1R including attenuation of excitotoxicity and modulating calcium ion flux in primary ganglion cells (Dun et al, 2007; Mueller et al, 2013). Compelling evidence that activation of Sig1R confers neuroprotection has been reported also in *in vivo* models of retinal disease. For example, targeting Sig1R has been investigated in retinal diseases such diabetic retinopathy (Smith et al, 2008, Wang et al, 2016a), ischemia reperfusion (Bucolo et al, 2006), and light-induced retinopathy (Shimazawa et al, 2015). The results have been uniformly promising. While the precise molecular mechanisms by which Sig1R activation mediates retinal neuroprotection are under active investigation, attenuation of oxidative stress especially through modulation of NRF2, has emerged as an important factor (Wang et al, 2019a, Wang et al 2015).

A retinal degeneration model that has proven valuable to investigate therapeutic properties of Sig1R activation and other intervention strategies is the *Pde6b*$^{rd10/J}$ (*rd10*) mouse. *Rd10* mice carry a spontaneous missense point mutation in exon 13 of the beta-subunit of the rod cGMP phosphodiesterase (β-PDE) gene (Chang et al, 2002; Chang et al, 2007). While the *rd10* retina is similar histologically to wildtype (WT) mice during the first two post-natal weeks (~P14), rod PRC loss begins at P18 and peaks at P25 (Gargini et al, 2007; Wang et al, 2017). Cone PRCs subsequently die; indeed by P35 only a single row of cones persist in the outer nuclear layer. The rapid course of the degeneration permits a defined window of time to assess treatments (Guadagni et al, 2015).

In initial studies with *rd10* mice, we determined that cone function, when assessed by ERG with a pseudorandom luminance ('natural') noise test, was vastly improved in *rd10* mice treated with the high-affinity, high-specificity Sig1R ligand (+)-pentazocine ((+)-PTZ) *v.* non-treated *rd10* mice at P35 (Wang et al, 2016b). Visual acuity of (+)-PTZ-treated *rd10* mice assessed using the optokinetic response (OKR) was significantly better than non-treated *rd10* mice. There was robust retention of acuity in (+)-PTZ-treated *rd10* mice through P56, which far surpassed the precipitous decline in non-treated mutant mice (Wang et al, 2019a). Other outcome measures supported the positive neuroprotective effects of activating Sig1R using an experimental protocol in which *rd10* mutant mice were administered (+)-PTZ via an intraperitoneal route beginning on P14 and continuing every other day until termination of the experiment. Initiating treatment at P14 (or at even younger ages) in *rd10* mice has been a common practice for a number interventional strategies (Piano et al, 2013; Zhu et al, 2020; Valdés-Sánchez 2019; Garces et al, 2020). This early intervention time point precedes frank disruption of the retina and is a sensible approach for testing therapeutic efficacy. It may not always be feasible, however, to intervene in retinopathies prior to disease onset. Indeed, patients may not know their disease status until manifestation of the clinical phenotype. Nonetheless, understanding optimal treatment regimen is highly desirable. Here we investigated whether delaying (+)-PTZ treatment would yield as robust a functional outcome in *rd10* mice as initiating the treatment during the pre-degenerative phase. To this end, we delayed onset of treatment until P18, P21 or P24 and compared the retinal function and structure to *rd10* mice whose treatment started at P14. Essentially, we were asking whether we can postpone the start of treatment by a few days in this severe disease model and still observe similar beneficial effects.

2. Methods

2.1. Animals

Breeding pairs of B6.CXBI-*Pde6βrd10/J* (*rd10*) mice were purchased from Jackson Laboratories (Bar Harbor, ME). Genotyping and the absence of *Crb1*$^{rd8/rd8}$ mutation were confirmed as described (Wang et al, 2016b). Oversight of the mouse colony followed our IACUC-approved protocol and was consistent with the ARVO statement for Use of Animals in Ophthalmic and Vision Research. Five groups of mice were evaluated over a period of 42 days, the groups differed based upon the post-natal day (P) when (+)-PTZ injections began: (1) *rd10* mice (non-treated), (2) *rd10*+PTZ (P14); (3) *rd10*+PTZ (P18); (4) *rd10*+PTZ (P21); (5) *rd10*+PTZ (P24). (+)-PTZ (Sigma-Aldrich, St. Louis, MO) was dissolved in DMSO and

0.01M PBS. It was administered via intraperitoneal (*i.p.*) injection (0.5 mg/kg) on alternate days beginning at P14, 18, 21, or 24. C57Bl/6 WT mice (Jackson Laboratories) were used for comparison in the ERG and SD-OCT studies (described below). Table 1 provides information on the numbers of mice used in the study.

2.2 Visual acuity assessment

Visual acuity, determined as spatial threshold for optokinetic tracking of sine-wave gratings, was measured in each mouse group at four time points: P21, P28, P35, P42. The OptoMotry system (CerebralMechanics, Medicine Hat, Alberta, Canada) was used following the initial method description (Prusky et al, 2004). As described in our earlier study (Navneet et al, 2019), vertical sine-wave gratings moving at 12°/s or gray of the same mean luminance are projected on four computer monitor screens that are attached and act as a virtual cylinder. The mouse is unrestrained on a pedestal at the epicenter of the cylinder. The responses are scored via live video using a method of limits procedure with a yes/no criterion. A spatial frequency (SF) threshold is generated at 100% contrast through each eye separately in the testing session.

2.3 Electroretinography (ERG)

To evaluate rod and cone function, mice were anesthetized at P35 by *i.p* injection of ketamine 80 mg/kg, xylazine 10 mg/kg. ERGs were performed using Touch/Touch feature of the Celeris Ophthalmic Electrophysiology System (Diagnosys, Lowell, MA). To ensure corneal moisture, 0.3% hypromellose solution was deposited in the cup of the electrode, which was placed on the cornea. The Touch/Touch protocol stimulates one eye at a time and uses the fellow, unstimulated eye as the reference. Mice were dark-adapted for approximately 16 hours prior to scotopic ERGs (rod function), which were tested using a series of light flashes of increasing energy (0.001, 0.005, 0.01, 0.1, 0.5, and 1.0 cd.s/m^2). Upon completion of dark-adapted testing, the light-adapted (photopic) testing program was initiated during which time rods were saturated using the adaptive light background feature of the Celeris system. The approximate light adaptation time for the Celeris system is approximately 2–5 minutes. Photopic testing was performed using flashes of 3, 10, 25, 50, 100, and 150 cd.s/m^2.

2.4. Spectral domain - optical coherence tomography (SD-OCT)

At P42, retinal structure was evaluated in mice (anesthetized by *i.p* injection of ketamine 80 mg/kg, xylazine 10 mg/kg) using the Bioptigen Spectral Domain Ophthalmic Imaging System (SDOIS; Bioptigen Envisu R2200, Durham, NC) as described previously (Navneet et al, 2019;Wang et al, 2016b; Wang et al, 2019b; Xiao et al, 2020). We used the manual caliper feature to measure the total retinal thickness, thickness of the inner retina and thickness of the outer retina as described previously (Wang et al, 2019a, Mezu-Ndubuisi et al, 2017). The inner retina measurement extended from the inner limiting membrane (ILM) to the distal edge of the inner nuclear layer (INL). The inner retina included the nerve fiber layer, ganglion cell layer, inner plexiform layer and the INL. The outer retina measurement extended from the distal edge of the INL to the basolateral border of the retinal pigment epithelium layer (RPE) and included the outer plexiform layer, outer nuclear layer (ONL), the inner and outer segments and the RPE. In instances where there was separation

(detachment) of PRCs from RPE, which is a common feature of the *rd10* retina, we measured the RPE layer thickness and added this value to the outer retinal thickness.

2.5 Morphometric analysis of retinas

Eyes were harvested from euthanized mice (age: P42). They were processed for embedding in JB-4 methacrylate or flash frozen for cryosectioning as described (Xiao et al, 2020). Sections were viewed using a Zeiss Axio Imager D2 microscope (Carl Zeiss, Göttingen, Germany) equipped with a high-resolution camera and processed using Zeiss Zen 2.3 Pro software. There is extensive PRC loss in the *rd10* mouse, therefore, we did not count rows of PRC nuclei, rather we counted the total number of PRC nuclei along the full length of retina (from the temporal to nasal ora serrata). Specifically, we counted cells in the three regions (central, mid-peripheral, peripheral regions) on the nasal and on the temporal side of the optic nerve and performed this morphometric analysis in three separate sections per mouse. Nuclei counts were averaged per mouse/per treatment group and were expressed as the number of PRC nuclei per 100μm retinal length. To evaluate whether cone PRCs were preserved, retinal cryosections were subjected to FITC-conjugated peanut agglutinin (PNA) (Millipore/Sigma), which selectively binds cone inner/outer segments. Retinal cryosections (10μm thickness) were fixed 10 min in 4% paraformaldehyde, blocked with Power Block (Bio-Genex, San Ramon, CA) diluted 1:10 for 1h at room temperature. All washing steps contained 0.1%Triton-X100/phosphate-buffered saline. Sections were incubated with FITC-PNA at a concentration of 1:100 overnight at 4°C. Retinas were examined by immunofluorescence using the Zeiss Axio Imager D2 microscope. Earlier reports showed increased PNA-labeling in *rd10* mice treated with (+)-PTZ beginning on P14 compared to non-treated mice (Wang et al, 2016b).

2.6. Data analysis

Statistical analysis used GraphPad Prism (version 8.0) analytical program (LaJolla, CA). Data were analyzed by one-way or two-way ANOVA followed by Tukey's test or Sidak's multiple comparison test as appropriate. Significance was set as $p<0.05$.

3. Results

3.1. Visual acuity assessment

Earlier work showed significant improvement in visual acuity in (+)-PTZ-treated *rd10* mice when Sig1R was activated beginning at P14 compared to non-treated mice (Wang et al, 2016b; Wang et al, 2019a; Xiao et al, 2020). To assess whether delaying the initial administration of (+)-PTZ (by a few days) would yield a similar positive outcome, we injected *rd10* mice with (+)-PTZ beginning at P18, P21 or P24 and compared the findings with *rd10* mice injected at P14 and to non-treated *rd10* mice. Visual acuity was evaluated in each cohort of mice at four time points: P21, P28, P35, P42. In *rd10*-non-treated mice the visual acuity was ~0.32 c/d at P21, ~0.37 c/d at P28; but decreased dramatically to ~0.13 at P35 and ~0.12 P42 (Fig. 1A). These findings are consistent with previous results for this mutant mouse. In contrast, *rd10* mice treated with (+)-PTZ beginning at P14 retained visual acuity through P42 (median visual acuity was ~0.33 c/d at P21, ~0.38 c/d at P28, ~0.32 c/d at P35, ~0.32 c/d at P42 (Fig. 1B). The visual acuity in mutant mice treated with (+)-PTZ

beginning at later time points was significantly better than non-injected *rd10* mice, however it was less robust compared to P14-injected mice, particularly when tested at P35 and P42. For example, in *rd10* mice injected beginning at P18 or at P21 visual acuity was ~0.3 when tested at P21 and P28, but it declined significantly when tested at P35 to ~0.23, and to ~0.15 at P42 (Fig. 1C and D). For *rd10* mice in which treatment began at P24, the visual acuity started to decrease when tested at P28 and was significantly reduced by P42 (~0.14 /d) (Fig. 1E), though was slightly better than non-treated *rd10* mice. The data suggest that initiating treatment with (+)-PTZ at P14 improves visual acuity in *rd10* mice; delaying the injection by a few days compromises effectiveness. The OKR data are presented individually in Figs. 1A–E and are combined in Fig. 1F.

3.2 ERG assessment of retinal function

Rd10 mice administered (+)-PTZ starting at P18, P21 or P24 on alternate days, were subjected to ERG analysis at P35 to assess cone (photopic) and rod (scotopic) function compared to age-matched, *rd10* mice in which (+)-PTZ injections began at P14 and to non-treated *rd10* mice. Regarding cone responses, representative light-adapted tracings are shown for responses to 5 flash intensities ranging from 3 to 150 cd.s/m^2. Examination of responses from non-treated *rd10* mice show minimal responses (Fig. 2A), whereas *rd10* mice treated with (+)-PTZ beginning at P14 demonstrated a much more robust response (Fig. 2B). The *rd10* mice in which (+)-PTZ treatment was delayed slightly had photopic responses that were somewhat better than non-treated animals (P18, Fig. 2C; P21, Fig. 2D; P24, Fig. 2E), but not to the extent as those administered (+)-PTZ at the P14 time point. The averaged photopic b-wave amplitude measured as the light-adapted ERG response was significantly greater in *rd10* mice administered (+)-PTZ beginning at P14 compared to non-treated *rd10* mice and to *rd10* mice administered (+)-PTZ beginning at P18, P21 or P24 (Fig. 2F). The data reflect more robust functional responses in mice treated at the earliest time point assessed in this study, but reduced responses in those for whom the treatment began several days later.

Regarding rod activity at P35, consistent with the profound loss of rod cells in *rd10* mice by this age, there was minimal detection of function at all but the highest light flash intensities. Representative dark-adapted ERG tracings for the highest luminance tested (1 cd.s/m^2) for mice in each of the 5 treatment groups are shown (Suppl. Fig. 1A). For comparison, a tracing from a WT mouse is shown (Suppl. Fig. 1A). WT mice frequently have b-wave amplitudes of 400–600μV, whereas the *rd10* mice had minimal responses. Indeed, for the mutants, the a-waves, indicative of rod PRC function are virtually non-detectable; b-waves, indicative of inner retinal function, are only slightly detectable. The average dark-adapted (scotopic) b-wave amplitudes are shown for mice in the four treatment groups and the b-wave amplitude is similar to non-injected *rd10* mice (Suppl. Fig. 1B). Thus, consistent with earlier reports (Wang et al, 2016b), (+)-PTZ treatment does not rescue rod function in *rd10* mice, but has a positive effect on cone function, especially if administered beginning at P14.

3.3. SD-OCT assessment of retinal architecture

Retinal structure of *rd10* mice administered (+)-PTZ starting at P18, P21 or P24 (and continuing every other day), were subjected to comprehensive SD-OCT analysis at P42

compared to *rd10* mice in which (+)-PTZ injections began at P14 and to non-treated *rd10* mice. Representative B-scans are shown for each group of mice in the study (Fig. 3A) and higher magnification images are also provided (Fig. 3B). The marked disruption of the outer retina of the *rd10* mouse precludes use of the auto segmentation post-imaging analysis feature of the Bioptigen Divers software, which is commonly used to measure retinal layers in less severe retinal degeneration models. Instead, we used the manual calipers feature of the Bioptigen system to measure the total retinal thickness, the thickness of the inner retina and the outer retina (delineation of these measurements is shown in Fig. 3B). We examined the retinas of age-matched WT mice for comparison. The total retinal thickness of WT measures ~220μm, and the inner and outer retina measure ~90μm and ~130μm, respectively (Fig. 3C). In contrast, the total retinal thickness in non-treated *rd10* mice was ~108μm; for mice injected at P18, P21 and P24 the total retinal thickness was ~107, ~110 and ~113μm, respectively (Fig. 3D). These values were significantly less than *rd10* mice injected at P14 (~125μm). It is known that the portion of retina most impacted in *rd10* mice is the outer region, which includes PRCs and inner/outer segments. The outer retina measured ~25μm in non-treated *rd10* mice, but was significantly greater (~35μm) in *rd10* mice in which (+)-PTZ injections began on P14 (Fig. 3E). The outer retina of mice in the other (+)-PTZ-injected groups (P18, P21, P24) measured ~25μm, which did not differ significantly from that of the non-treated *rd10* mice (Fig. 3E). The inner retina is less affected in *rd10* mice. At P42, it typically measures ~85μm (in non-treated *rd10* mice), which is only slightly less than WT mice (~90μm). In the (+)-PTZ-treated mice there was significant increase in the *rd10* mice injected with (+)-PTZ on P14 (~89μm), whereas inner retinal thickness remained similar to non-treated in those *rd10* mice administered (+)-PTZ beyond P14 (Fig. 3F).

3.4. Histologic assessment

Following the vision function analyses, eyes were harvested at P42 from *rd10* mice administered (+)-PTZ starting at P18, P21 or P24 (and continuing on alternate days) and were processed for embedding in JB-4 methacrylate. Representative hematoxylin-eosin stained sections of retinas from mice in each treatment group are provided (Fig. 4). Comparisons were made to non-treated *rd10* mice and to mice administered (+)-PTZ beginning at P14 (with (+)-PTZ treatment continuing also on alternate days). Regarding the inner retina, the cellular and synaptic layers are clearly evident in non-treated *rd10* mice (Fig. 4A) as well as the (+)-PTZ-treated mice, regardless of the day (+)-PTZ treatment was initiated (Fig. 4B–E). That is, the inner plexiform layer and INL are clearly discernable. In contrast, the outer retina is considerably reduced in thickness in non-treated *rd10* mice. Aside from a single layer of cells in the outer nuclear layer (ONL) (arrows, Fig. 4A), the inner and outer segments are not detectable in non-treated *rd10* retinas. Measurement of the number of PRC nuclei in the ONL of non-treated *rd10* mice yields ~10 PRC nuclei/100μm retinal length (Fig. 4F). Retinas of *rd10* mice in which (+)-PTZ treatment began at P14 typically had 2 (and sometimes 3) rows of PRC nuclei within the ONL (Fig. 4B, arrows). In these (+)-PTZ-treated *rd10* mice, there were ~20 PRC nuclei/100μm retinal length, which was significantly greater than the non-treated mice. Furthermore, it was significantly greater than mice in the delayed treatment groups ((+)-PTZ starting at P18 (~16 nuclei/100μm), P21 (~17 nuclei/100μm), P24 (~15 nuclei/100μm) (Fig. 4F). For the mice in the delayed treatment groups there was typically ~1 (and sometimes 2) rows of cells in the ONL (Figs.

4C–E, arrows). There were significantly more nuclei per 100μm retinal length in the P18, P21 and P24-injected mice than non-treated mice (Fig. 4F).

Evaluation of retinal cryosections using FITC-conjugated PNA, a marker for cones, showed robust labeling in WT mice (Fig. 5A, arrow) but very limited labeling in non-treated *rd10* mice (Fig. 5B). Cone labeling was evident in retinas of mice administered (+)-PTZ at P14 (Fig. 5C) as well as at P18 (Fig. 5D), P21 (Fig. 5E), and P24 (Fig. 5F). The data suggest that the majority of cells present in the ONL shown in Fig. 4 are likely cone PRCs.

4. Discussion

In this study we evaluated the relevance of the timing of treatment on therapeutic outcome in a severe retinal disease model. We compared consequences of administering (+)-PTZ prior to, during and following rod PRC loss in the *rd10* mouse, a model well-suited for therapeutic optimization analysis (Gargini et al, 2007; Guadagni et al, 2015). P14 represents a time point prior to PRC death. P18 coincides with the onset of PRC death in *rd10* mice (Doonan et al, 2011). At P21 the *rd10* retina is ~150μm thick and has ~8 rows of PRC nuclei in the ONL compared to 10–12 rows in WT retina. At P24 the *rd10* retina is ~100μm thick and there are ~5–6 rows of cells in the ONL. Thus, P21 and P24 represent time points of active PRC degeneration, especially rod PRCs.

Our investigation involved functional retinal assessments including visual acuity measurements, which were improved in *rd10* mice administered (+)-PTZ beginning at either P14, 18, 21 or 24 compared to non-treated *rd10* mice. However, the improvement in mice injected at P14 was considerably better than in mice for which the administration began at or following PRC degeneration (i.e. P18 or later). The outcome of other functional tests was less robust for later onset administration times. Photopic ERG responses were significantly better in animals injected at P14 compared with the other groups. Similarly, OCT measurements of either the entire retinal thickness or the outer retinal thickness were improved significantly in the P14-injected group, but not in the later-injection groups. The OCT findings were consistent with the histologic analysis (at P42), which showed ~2 rows of PRCs remaining in the *rd10* mice injected beginning at P14 but only ~1 row of cells in the groups for which (+)-PTZ injection was delayed.

A number of studies have used the *rd10* mouse and evaluated therapeutic potential of promising compounds. Studies involving the progesterone analogue norgestrel reported that i.p. administration at P18 in *rd10* mice attenuated death of cells in the ONL (Doonan et al, 2011). Several studies have been reported in which the pharmacologic treatment in *rd10* mice commenced prior to P18, the onset of rod death, and were often accompanied by favorable outcomes. For example, administration of ITH12674, a compound that induces NRF2 transcription, to *rd10* mice beginning at P16 resulted in improved visual acuity and preservation of cone PRCs compared to non-treated mutant mice (Campello et al, 2020); administration of a MyD88 inhibitor at P14 in the *rd10* mice improved ERG responses at P25 (Garces et al, 2020); and twice daily administration of myriocin, a known inhibitor of serine–palmitoyl transferase, beginning at P14 resulted in cone PRCs, the inner retina and overall visual performance being preserved in *rd10* mice well after rod death (Piano et al,

2013). Treatment of *rd10* mice with metripranolol, a β-adrenergic receptor antagonist, beginning at P14 had promising effects in sustaining cone function through P65 (Kanan et al, 2019). This study actually compared systemic injections and topical (eyedrop) administration of metripranolol with very beneficial effects. Treatment of *rd10* mice with a resveratrol prodrug beginning at P13 preserved ERG function for at least 15 days (Valdés-Sánchez et al, 2019) and the potent antioxidant compound DHAG ((Z)-7,4'-dimethoxy-6-hydroxy-aurone-4-O-β-glucopyranoside) was effective in preserving retinal morphology, reducing PRC death and decreasing oxidative stress in *rd10* mice when administered beginning at P12 (Chen et al, 2020). Taken collectively, experimental paradigms in which *rd10* mice are treated early in the degenerative process appear more likely to yield a longer period of retinal function than those treated later. Whether this observation is generalizable to other retinal degeneration models, especially those that have a more slowly progressing degenerative phenotype such as the P23H opsin mutation (Sakami et al, 2011) remains to be tested, but slower degeneration models are likely to afford a much broader window of therapeutic intervention.

There has been an intriguing report of dietary manipulation in *rd10* mice that was initiated much later in the degenerative process. This study involved dietary supplementation with norgestrel beginning at P30 (substantially past the peak of rod cell death (P25)); the authors report retention of cone synaptic connectivity in the outer plexiform layer (Roche et al, 2019). The authors were cautiously hopeful that norgestrel may prove useful as a mid-stage treatment for retinal disease. Aside from the dietary supplementation studies, none of the aforementioned studies reported results for administration of test compounds at time points immediately following the frank onset of PRC loss as we describe here.

Our findings show that delayed (+)-PTZ injection – even by just a few days in *rd10* mice – can negatively impact the long-term preservation of retinal function. This finding has clinical and mechanistic relevance. Clinically, the data demonstrate that optimizing the administration of Sig1R ligands is critical for retinal neuroprotection. Delaying treatment to a point when cell death is accelerating appears to overwhelm the therapeutic potential of activating Sig1R. The observation is relevant to findings in human patients. Merkland and colleagues reviewed ophthalmic care in a group of Swedish patients and found a clear association between long waiting times for intervention and negative visual outcomes (Merkland et al, 2019). While it seems logical that timely treatment would be associated with patients' improved visual outcome our study provides empirical evidence in support of this practice.

Mechanistically, the data suggest that (+)-PTZ delays postnatal death of PRCs, particularly cones. It may do so by acting directly on cones or it may impact neighboring supportive cells (such as Müller glial cells), this remains to be investigated. In addition, activating Sig1R may be neuroprotective (in either or both of these retinal cell types) by mitigating oxidative stress, which is characteristic of the *rd10* retina (Campochiaro et al, 2018). Earlier reports that (+)-PTZ can increase levels of the antioxidant transcription factor NRF2 are consistent with this notion (Wang et al, 2019b). There are a host of other hypotheses as to the mechanism by which Sig1R confers neuroprotection in retina and other tissues such as brain. These include calcium modulation and reducing ER stress. Whether the *rd10* mouse

model with its very rapid progression will allow dissection of these various mechanisms is unclear. Again, it may be necessary to utilize more slowly progressing retinal degenerative models to make this determination.

One question that was not addressed in this study and has not been explored with respect to (+)-PTZ treatment in retinopathy is the potential of combinatorial treatment strategies. Examples might include targeted gene therapy combined with (+)-PTZ treatment or administering antioxidant therapies in conjunction with (+)-PTZ. It is well known that in severe retinal disease there can be considerable oxidative and ER stress compromising the retinal milieu, which may in turn limit effectiveness of novel therapies. For example, in targeted gene therapy, a specific cell may have its genetic defect repaired, but success of treatment may be compromised if the overall environment is unfavorable due to excessive oxidative stress, ER stress, inflammation etc. There is considerable evidence that targeting Sig1R reduces oxidative and ER stress. If used in concert with another treatment strategy, targeting Sig1R might promote a more favorable environment for novel therapeutic treatments (e.g. gene therapy). Designing and implementing these complex therapeutic strategies would be a very fruitful area of future studies.

Supplementary Material

Refer to Web version on PubMed Central for supplementary material.

Acknowledgements

This work was supported by the NIH (R01EY028103) and the Foundation Fighting Blindness (TA-NMT-0617-0721-AUG), and National Eye Institute P30 Center Core Grant for Vision Research (P30 EY031631). We thank Ms. Donna Kumiski for excellent technical support in preparing retinal histology sections.

References

Bucolo C, Marrazzo A, Ronsisvalle S, Ronsisvalle G, Cuzzocrea S, Mazzon E, Caputi A, Drago F. A novel adamantane derivative attenuates retinal ischemia-reperfusion damage in the rat retina through sigma1 receptors. Eur J Pharmacol. 2006;536:200–203. [PubMed: 16580663]

Campello L, Kutsyr O, Noailles A, et al. New Nrf2-Inducer Compound ITH12674 Slows the Progression of Retinitis Pigmentosa in the Mouse Model rd10. Cell Physiol Biochem. 2020;54:142–159. [PubMed: 32028545]

Campochiaro PA, Mir TA. The mechanism of cone cell death in Retinitis Pigmentosa. Prog Retin Eye Res. 2018;62:24–37 [PubMed: 28962928]

Carullo G, Federico S, Relitti N, Gemma S, Butini S, Campiani G. Retinitis Pigmentosa and Retinal Degenerations: Deciphering Pathways and Targets for Drug Discovery and Development. ACS Chem Neurosci. 2020;11:2173–2191. [PubMed: 32589402]

Chang B, Hawes NL, Hurd RE, Davisson MT, Nusinowitz S, Heckenlively JR. Retinal degeneration mutants in the mouse. Vision Res. 2002;42:517–525. [PubMed: 11853768]

Chang B, Hawes NL, Pardue MT, German AM, Hurd RE, Davisson MT, Nusinowitz S, Rengarajan K, Boyd AP, Sidney SS, Phillips MJ, Stewart RE, Chaudhury R, Nickerson JM, Heckenlively JR, Boatright JH. Two mouse retinal degenerations caused by missense mutations in the beta-subunit of rod cGMP phosphodiesterase gene. Vision Res. 2007;47:624–633. [PubMed: 17267005]

Chen Y, Yang M, Wang ZJ. (Z)-7,4'-Dimethoxy-6-hydroxy-aurone-4-O-β-glucopyranoside mitigates retinal degeneration in Rd10 mouse model through inhibiting oxidative stress and inflammatory responses. Cutan Ocul Toxicol. 2020;39:36–42. [PubMed: 31648555]

Doonan F, O'Driscoll C, Kenna P, Cotter TG. Enhancing survival of photoreceptor cells in vivo using the synthetic progestin Norgestrel. J Neurochem. 2011;118:915–927. [PubMed: 21689103]

Dun Y, Thangaraju M, Prasad P, Ganapathy V, Smith SB. Prevention of excitotoxicity in primary retinal ganglion cells by (+)-pentazocine, a sigma receptor-1 specific ligand. Invest Ophthalmol Vis Sci. 2007;48:4785–4794. [PubMed: 17898305]

Garces K, Carmy T, Illiano P, Brambilla R, Hackam AS. Increased Neuroprotective Microglia and Photoreceptor Survival in the Retina from a Peptide Inhibitor of Myeloid Differentiation Factor 88 (MyD88). J Mol Neurosci. 2020;70:968–980. [PubMed: 32072483]

Gargini C, Terzibasi E, Mazzoni F, Strettoi E. Retinal organization in the retinal degeneration 10 (rd10) mutant mouse: a morphological and ERG study. J Comp Neurol. 2007;500:222–238. [PubMed: 17111372]

Guadagni V, Novelli E, Piano I, Gargini C, Strettoi E. Pharmacological approaches to retinitis pigmentosa: A laboratory perspective. Prog Retin Eye Res. 2015;48:62–81. [PubMed: 26113212]

Jiang G, Mysona B, Dun Y, Gnana-Prakasam JP, Pabla N, Li W, Dong Z, Ganapathy V, Smith SB. Expression, subcellular localization, and regulation of sigma receptor in retinal muller cells. Invest Ophthalmol Vis Sci. 2006;47:5576–55 [PubMed: 17122151]

Kanan Y, Khan M, Lorenc VE, Long D, Chadha R, Sciamanna J, Green K, Campochiaro PA. Metipranolol promotes structure and function of retinal photoreceptors in the rd10 mouse model of human retinitis pigmentosa. J Neurochem. 2019;148:307–318. [PubMed: 30315650]

Mavlyutov TA, Epstein M, Guo LW. Subcellular localization of the sigma-1 receptor in retinal neurons - an electron microscopy study. Sci Rep. 2015;5:10689. [PubMed: 26033680]

Merkland D, Gjötterberg M. Care delay the most common error in ophthalmic health care. Lakartidningen. 2019;116:FSMU.

Mezu-Ndubuisi OJ, Taylor LK, Schoephoerster JA. Simultaneous Fluorescein Angiography and Spectral Domain Optical Coherence Tomography Correlate Retinal Thickness Changes to Vascular Abnormalities in an In Vivo Mouse Model of Retinopathy of Prematurity. J Ophthalmol. 2017:9620876. [PubMed: 28573047]

Mueller BH, Park Y, Daudt DR 3rd, Ma HY, Akopova I, Stankowska DL, Clark AF, Yorio T. Sigma-1 receptor stimulation attenuates calcium influx through activated L-type Voltage Gated Calcium Channels in purified retinal ganglion cells. Exp Eye Res. 2013;107: 21–31. [PubMed: 23183135]

Navneet S, Zhao J, Wang J, Mysona B, Barwick S, Ammal Kaidery N, Saul A, Kaddour-Djebbar I, Bollag WB, Thomas B, Bollinger KE, Smith SB. Hyperhomocysteinemia-induced death of retinal ganglion cells: The role of Müller glial cells and NRF2. Redox Biol. 2019;24:101199. [PubMed: 31026769]

Nguyen L, Lucke-Wold BP, Mookerjee SA, Cavendish JZ, Robson MJ, Scandinaro AL, Matsumoto RR. Role of sigma-1 receptors in neurodegenerative diseases. J Pharmacol Sci. 2015;127:17–29. [PubMed: 25704014]

Ola MS, Moore P, El-Sherbeny A, Roon P, Agarwal N, Sarthy VP, Casellas P, Ganapathy V, Smith SB. Expression pattern of sigma receptor 1 mRNA and protein in mammalian retina. Brain Res Mol Brain Res. 2001;95:86–95. [PubMed: 11687279]

Piano I, Novelli E, Gasco P, Ghidoni R, Strettoi E, Gargini C. Cone survival and preservation of visual acuity in an animal model of retinal degeneration. Eur J Neurosci. 2013;37:1853–1862. [PubMed: 23551187]

Prusky GT, Alam NM, Beekman S, Douglas RM. Rapid quantification of adult and developing mouse spatial vision using a virtual optomotor system. Invest Ophthalmol Vis Sci. 2004;45:4611–4616. [PubMed: 15557474]

Roche SL, Kutsyr O, Cuenca N, Cotter TG. Norgestrel, a Progesterone Analogue, Promotes Significant Long-Term Neuroprotection of Cone Photoreceptors in a Mouse Model of Retinal Disease. Invest Ophthalmol Vis Sci. 2019;60:3221–3235. [PubMed: 31335948]

Sakami S, Maeda T, Bereta G, Okano K, Golczak M, Sumaroka A, Roman AJ, Cideciyan AV, Jacobson SG, Palczewski K. Probing mechanisms of photoreceptor degeneration in a new mouse model of the common form of autosomal dominant retinitis pigmentosa due to P23H opsin mutations. J Biol Chem. 2011;286:10551–10567. [PubMed: 21224384]

Shimazawa M, Sugitani S, Inoue Y, Tsuruma K, Hara H. Effect of a sigma-1 receptor agonist, cutamesine dihydrochloride (SA4503), on photoreceptor cell death against light-induced damage. Exp Eye Res. 2015;132:64–72. [PubMed: 25616094]

Smith SB, Duplantier J, Dun Y, Mysona B, Roon P, Martin PM, Ganapathy V. In vivo protection against retinal neurodegeneration by sigma receptor 1 ligand (+)-pentazocine. Invest Ophthalmol Vis Sci. 2008;49:4154–4161. [PubMed: 18469181]

Smith SB, Wang J, Cui X, Mysona BA, Zhao J, Bollinger KE. Sigma 1 receptor: A novel therapeutic target in retinal disease. Prog Retin Eye Res. 2018;67:130–149. [PubMed: 30075336]

Su TP, Su TC, Nakamura Y, Tsai SY. The Sigma-1 Receptor as a Pluripotent Modulator in Living Systems. Trends Pharmacol Sci. 2016;37:262–78. [PubMed: 26869505]

Valdés-Sánchez L, García-Delgado AB, Montero-Sánchez A, et al. The Resveratrol Prodrug JC19 Delays Retinal Degeneration in rd10 Mice. Adv Exp Med Biol. 2019;1185:457–462. [PubMed: 31884654]

Wang J, Cui X, Roon P, Smith SB. Role of Sigma 1 Receptor in Retinal Degeneration of the Ins2Akita/+ Murine Model of Diabetic Retinopathy. Invest Ophthalmol Vis Sci. 2016;57:2770–2781. (a) [PubMed: 27206247]

Wang J, Saul A, Cui X, Roon P, Smith SB. Absence of Sigma 1 Receptor Accelerates Photoreceptor Cell Death in a Murine Model of Retinitis Pigmentosa. Invest Ophthalmol Vis Sci. 2017;58:4545–4558. [PubMed: 28877319]

Wang J, Saul A, Roon P, Smith SB. Activation of the molecular chaperone, sigma 1 receptor, preserves cone function in a murine model of inherited retinal degeneration. Proc Natl Acad Sci U S A. 2016;113:E3764–3772. (b) [PubMed: 27298364]

Wang J, Saul A, Smith SB. Activation of Sigma 1 Receptor Extends Survival of Cones and Improves Visual Acuity in a Murine Model of Retinitis Pigmentosa. Invest Ophthalmol Vis Sci. 2019;60:4397–4407. (a) [PubMed: 31639826]

Wang J, Shanmugam A, Markand S, Zorrilla E, Ganapathy V, Smith SB. Sigma 1 receptor regulates the oxidative stress response in primary retinal Müller glial cells via NRF2 signaling and system xc(−), the Na(+)-independent glutamate-cystine exchanger. Free Radic Biol Med. 2015; 86:25–36. [PubMed: 25920363]

Wang J, Zhao J, Cui X, Mysona BA, Navneet S, Saul A, Ahuja M, Lambert N, Gazaryan IG, Thomas B, Bollinger KE, Smith SB. The molecular chaperone sigma 1 receptor mediates rescue of retinal cone photoreceptor cells via modulation of NRF2. Free Radic Biol Med. 2019;134:604–616. (b) [PubMed: 30743048]

Xiao H, Wang J, Saul A, Smith SB. Comparison of Neuroprotective Effects of Monomethylfumarate to the Sigma 1 Receptor Ligand (+)-Pentazocine in a Murine Model of Retinitis Pigmentosa. Invest Ophthalmol Vis Sci. 2020;61:5.

Zhu D, Xie M, Gademann F, et al. Protective effects of human iPS-derived retinal pigmented epithelial cells on retinal degenerative disease. Stem Cell Res Ther. 2020;11:98. [PubMed: 32131893]

Highlights

- The Sig1R ligand (+) pentazocine ((+)-PTZ) is neuroprotective in the *rd10* mouse model of RP
- Administering (+)-PTZ prior to onset of PRC death delays cone loss and extends visual acuity
- Delaying (+)-PTZ injection past onset of PRC death negatively impacts retinal function in *rd10* mice
- Optimizing Sig1R ligand administration is critical for retinal neuroprotection

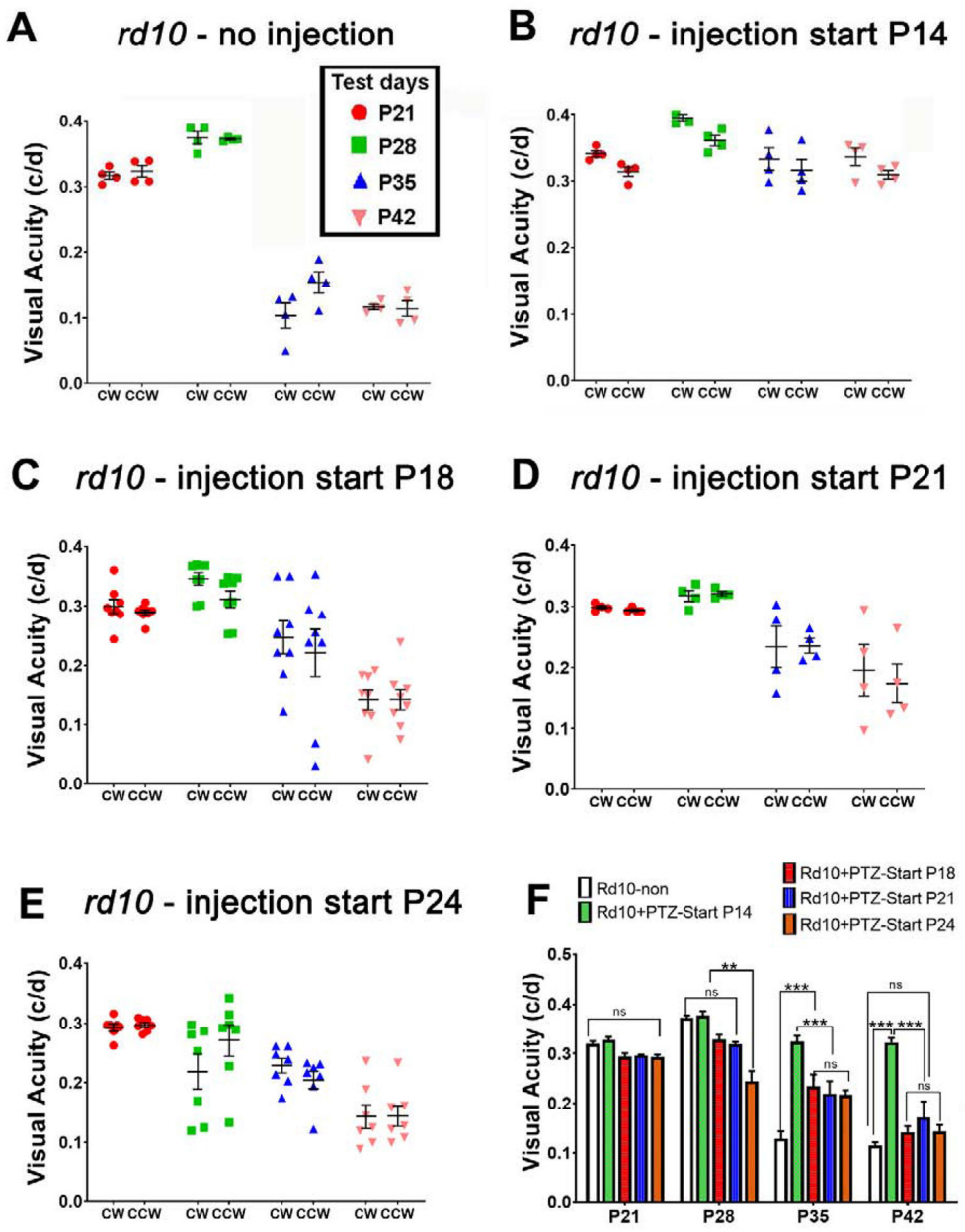

Figure 1. Assessment of visual acuity.

Rd10 mice were administered (+)-PTZ every other day beginning at P14, P18, P21, or P24 and were compared to non-treated *rd10* mice. The optokinetic tracking response (OKR) was measured using the OptoMotry system to assess visual acuity over the age range of P21, P28, P35 and P42. Data are expressed as cycles/degree (c/d) for (A) non-treated *rd10* mice, and (+)-PTZ-treated *rd10* mice beginning at (B) P14, (C) P18, (D) P21, (E) P24. Data are mean ± SEM and were analyzed by two-way ANOVA and are summarized for comparison in panel (F). Significance is depicted as: $^{**}p < 0.01$, $^{***}p < 0.001$, ns = not significant. (CW = left eye, CCW = right eye.)

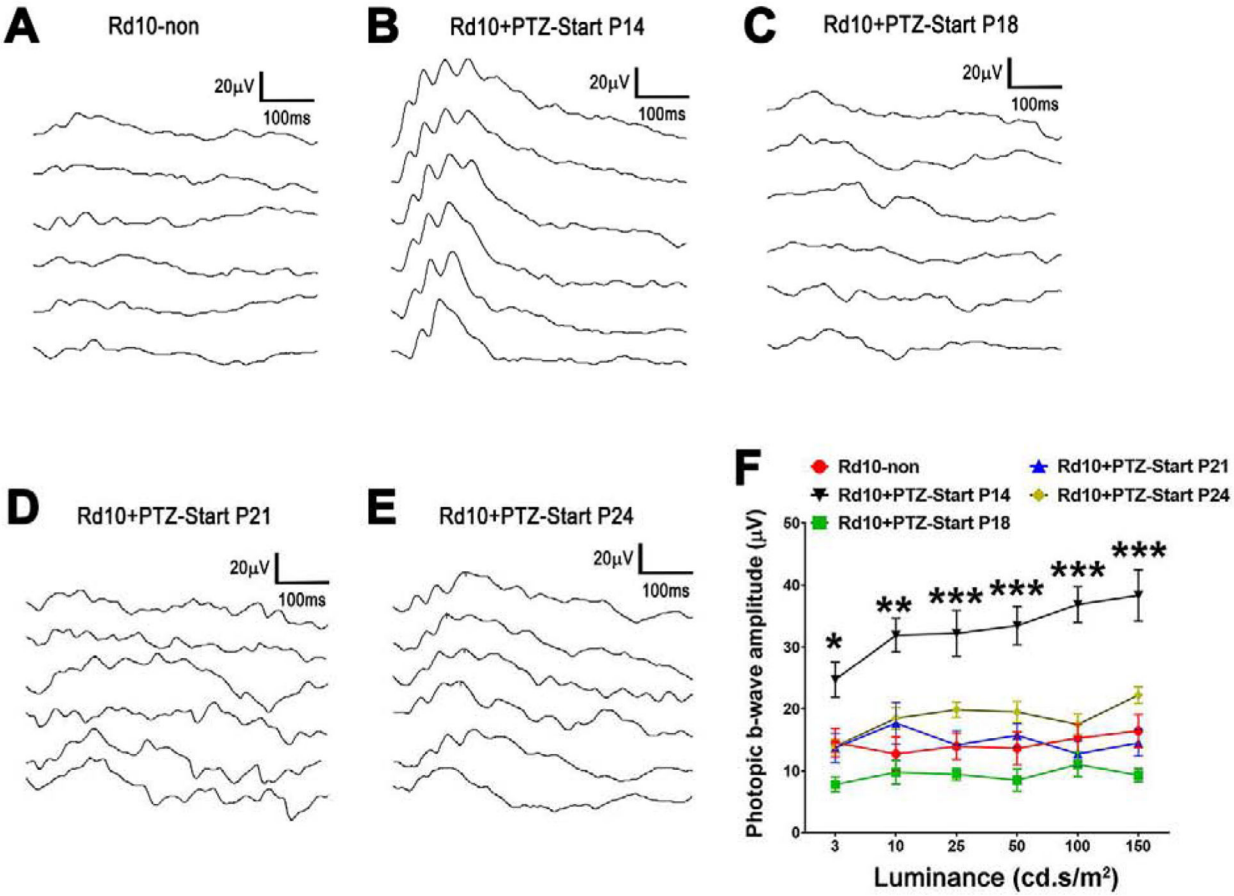

Figure 2. Assessment of retinal function by photopic ERG.

Rd10 mice were administered (+)-PTZ every other day beginning at P14, P18, P21, or P24 and were compared to non-treated *rd10* mice. Photopic ERG responses were evaluated at P35. Representative photopic ERG responses at five stimulus contrasts for (A) *rd10*-non injected, and *rd10* mice injected beginning at (B) P14, (C) P18, (D) P21, (E) P24. (F) Averaged photopic b-wave amplitude responses to a series of intensities of flash energy (3, 10, 25, 50, 100 and 150 cd.s/m^2). Intensities were in units of candela-seconds per meter squared (cd.s/m^2). Data are mean ± SEM and were analyzed by two-way ANOVA, significance is depicted as *p<0.05; **p< 0.01; ***p< 0.001.

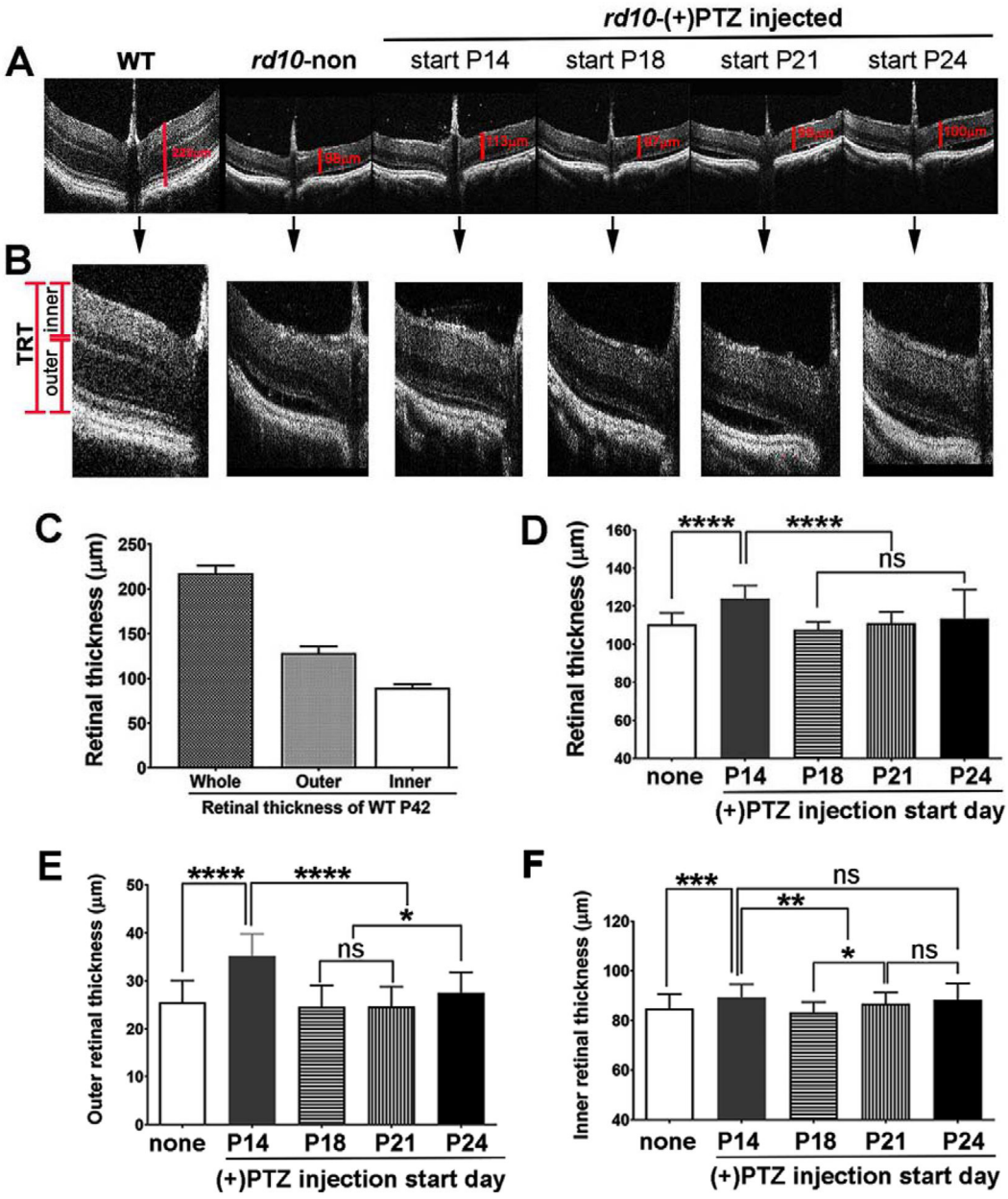

Figure 3. Assessment of retinal structure in vivo using SD-OCT.

(A) Representative SD-OCT images are shown for WT mice and *rd10* mice administered (+)-PTZ beginning at P14, P18, P21, or P24 vs. non-treated *rd10* mice. SD-OCT was performed at P42. (B) Higher magnification images of retinas of WT mice and *rd10* mice administered (+)-PTZ beginning at P14, P18, P21, or P24 vs. non-treated *rd10* mice. Red markers (left side of panel B) show the measurement endpoints for total retinal thickness (TRT), outer and inner retina. Data from analysis of (C) total retinal thickness and inner/outer retinal thickness in WT mice, (D) total retinal thickness, (E) outer retinal thickness, (F) inner retinal thickness of *rd10* mice administered (+)-PTZ beginning P14, P18, P21, or P24 vs. non-treated *Rd10* mice. Data are mean ± SEM and were analyzed by one-way ANOVA, significance is depicted as *p<0.05; **p< 0.01; ***p< 0.001, ns= not significant.

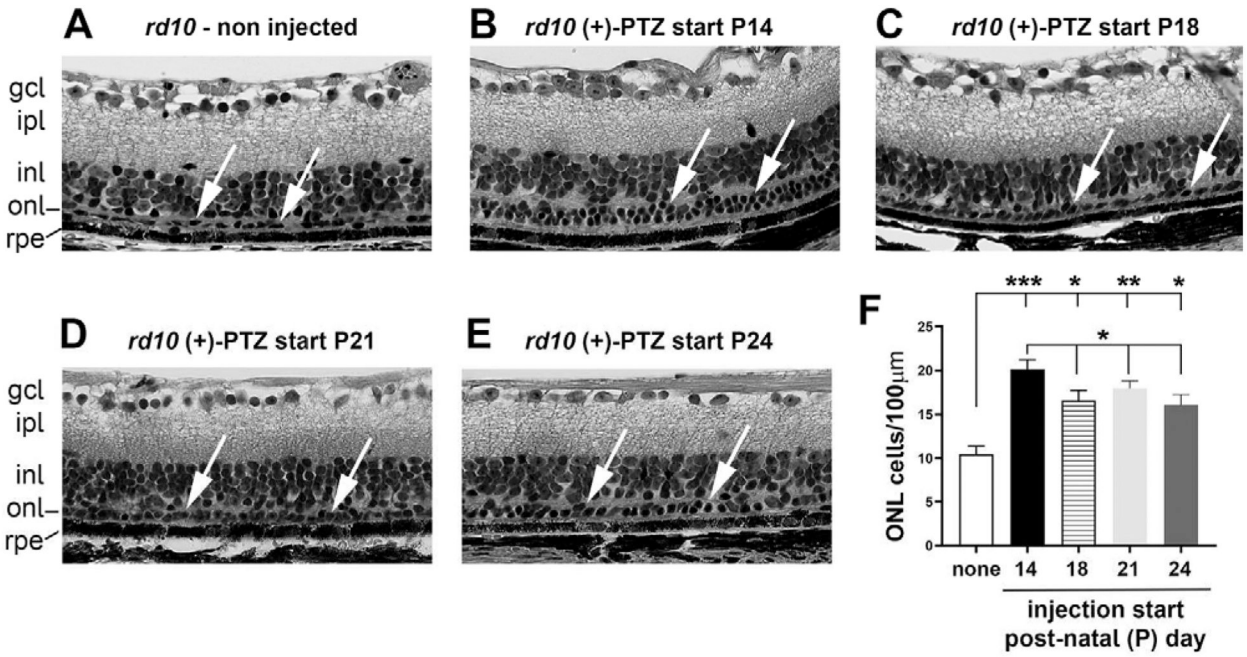

Figure 4. Morphologic and morphometric assessment.

Following the *in vivo* studies, one eye per mouse was processed for embedding in JB-4 plastic. Sections were stained with hematoxylin and eosin. Representative photomicrographs are shown for (A) non-treated *rd10* mouse, or *rd10* mice administered (+)-PTZ starting on (B) P14, (C) P18, (D) P21, (E) P24. Given the severity of the degeneration it was impractical to count rows of PRC nuclei. Thus, the total number of cells in the ONL was counted and expressed as cells/100μm retinal length. Data are mean ± SEM and were analyzed by one-way ANOVA, significance is depicted as *p<0.05; **p< 0.01; ***p< 0.001, ns= not significant.

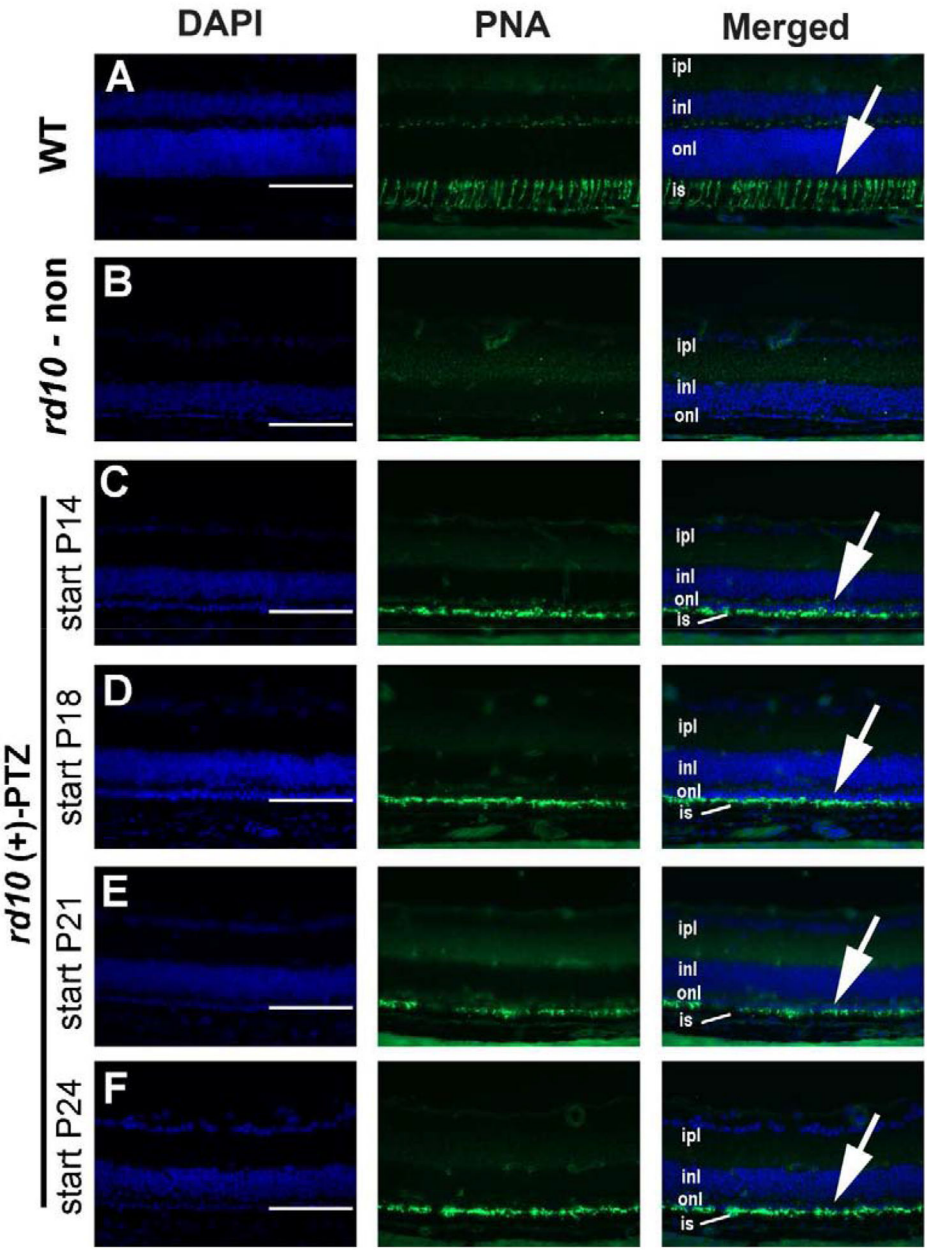

Figure 5. Evaluation of cone photoreceptor labeling.

Following the *in vivo* studies, one eye per mouse was processed for cryosectioning and immunodetection of FITC-conjugated peanut agglutinin (PNA), a green fluorescent marker of cone PRCs. Representative photomicrographs are shown for (A) WT, (B) non-treated *rd10* mouse, or *rd10* mice administered (+)-PTZ starting on (C) P14, (D) P18, (E) P21, (F) P24. (Arrows in A, C-F point to green fluorescing cone inner segments.) Abbreviations: ipl, inner plexiform layer; inl, inner nuclear layer; onl, outer nuclear layer; is, inner segments. Calibration bar = 100μm.

Table 1.

Number of animals used in the study.

Mouse Group	N	Age (post-natal days)
ERG analysis		
WT	4	35
Rd10 (0.5 mg kg-1 (+)-PTZ-start P14)	7	35
Rd10 (0.5 mg kg-1 (+)-PTZ-start P18))	8	35
Rd10 (0.5 mg kg-1 (+)-PTZ-start P21)	4	35
Rd10 (0.5 mg kg-1 (+)-PTZ-start P24)	7	35
OCT analysis		
WT	4	42
Rd10	7	42
Rd10 (0.5 mg kg-1 (+)-PTZ-start P14)	7	42
Rd10 (0.5 mg kg-1 (+)-PTZ-start P18)	8	42
Rd10 (0.5 mg kg-1 (+)-PTZ-start P21)	4	42
Rd10 (0.5 mg kg-1 (+)-PTZ-start P24)	7	42
OKR analysis		
Rd10	4	21, 28, 35, 42
Rd10 (0.5 mg kg-1 (+)-PTZ-start P14)	4	21, 28, 35, 42
Rd10 (0.5 mg kg-1 (+)-PTZ-start P18)	8	21, 28, 35, 42
Rd10 (0.5 mg kg-1 (+)-PTZ-start P21)	4	21, 28, 35, 42
Rd10 (0.5 mg kg-1 (+)-PTZ-start P24)	7	21, 28, 35, 42
Morphometric analysis		
Rd10	7	42
Rd10 (0.5 mg kg-1 (+)-PTZ-start P14)	7	42
Rd10 (0.5 mg kg-1 (+)-PTZ-start P18)	8	42
Rd10 (0.5 mg kg-1 (+)-PTZ-start P21)	4	42
Rd10 (0.5 mg kg-1 (+)-PTZ-start P24)	7	42